

# Learning Robotic Policy with Imagined Transition: Mitigating the Trade-off between Robustness and Optimality

Wei Xiao, Shangke Lyu\*, Zhefei Gong, Renjie Wang, Donglin Wang\*

**Abstract**—Existing quadrupedal locomotion learning paradigms usually rely on extensive domain randomization to alleviate the sim2real gap and enhance robustness. It trains policies with a wide range of environment parameters and sensor noises to perform reliably under uncertainty. However, since optimal performance under ideal conditions often conflicts with the need to handle worst-case scenarios, there is a trade-off between optimality and robustness. This trade-off forces the learned policy to prioritize stability in diverse and challenging conditions over efficiency and accuracy in ideal ones, leading to overly conservative behaviors that sacrifice peak performance. In this paper, we propose a two-stage framework that mitigates this trade-off by integrating policy learning with imagined transitions. This framework enhances the conventional reinforcement learning (RL) approach by incorporating imagined transitions as demonstrative inputs. These imagined transitions are derived from an optimal policy and a dynamics model operating within an idealized setting. Our findings indicate that this approach significantly mitigates the domain randomization-induced negative impact of existing RL algorithms. It leads to accelerated training, reduced tracking errors within the distribution, and enhanced robustness outside the distribution.

## I. INTRODUCTION

Learning-based locomotion control methods for quadruped robots have achieved remarkable results in recent years [1], [2], [3], [4], [5], [6]. To adapt to various wild environments, these methods collected large amounts of data in massive parallel simulators with various dynamics and terrains for policy training via domain randomization [7] and curriculum learning [8]. This data-driven paradigm allows RL-based robots to adapt to realistic terrain and complex behavior commands.

Domain randomization is a vital technique to ensure the policy’s robustness. However, previous research [9], [10] found that it trades optimality for robustness and leads to conservative policies. In Figure 1, we observe that locomotion policies trained using modern RL algorithms can rapidly achieve high performance in simulators with fixed dynamics, provided that robustness and the sim2real gap are not considered. When robustness is incorporated into the training process, the resulting policies tend to exhibit more conservative behaviors, leading to lower cumulative rewards during training and reduced body height during deployment, as a precaution against unforeseen perturbations. **There exists a trade-off between optimality and robustness in current RL-based locomotion paradigms.**

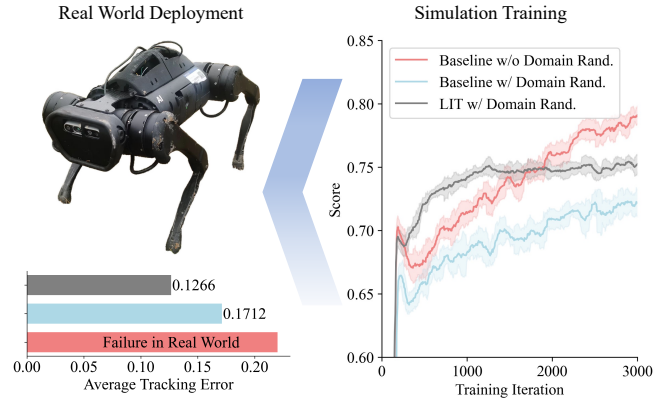


Fig. 1. Proposed LIT has lower tracking error than baseline. For current RL-based locomotion paradigms (Baseline), domain randomization trades optimality for robustness.

This phenomenon is caused by the large amount of randomness introduced by domain randomization, which greatly increases the exploration space of policy training. In addition, this is a Partially Observable Markov Decision Process (POMDP) problem [11], [12], and the agent cannot obtain all the environmental parameters. Therefore, the behavior of policies tends to be conservative to cope with unknown disturbances. However, this conservatism leads to a decrease in training efficiency because the robot is difficult to obtain high rewards during training. Therefore, we need a method to mitigate this phenomenon to balance optimality and robustness better.

In the training paradigm of robotic policies, we always hope that the robot operates according to a certain pattern. For example, in manipulation tasks, it is desired that the robotic arm accurately follows a trajectory. In the locomotion of quadruped robots, it is desired that a specific gait (e.g., trotting, walking, running, etc.) is maintained. We hope that this behavior pattern can remain consistent when facing different environmental parameters and disturbances. For quadrupedal robots, the desired gait in undisturbed simulators is easy to obtain via RL training without dynamics randomization, but it is difficult to maintain robustness when deployed in complex, real-world environments. However, the ideal gait can be used as a reference to guide the learning of robust policies in complex environments. To achieve this goal, we propose **LIT (Learning with Imagined Transition)**, a two-stage framework training paradigm that enables the learning of robust locomotion policies from ideal gait.

To get a gait like the one ideally trained in an undisturbed environment, we need to compress the action and observation

All the authors are with Machine Intelligence Lab (MiLAB), School of Engineering, Westlake University, Hangzhou 310024, China.

\*Corresponding author.

corresponding to the optimal gait into the neural network. This stage is called reference learning in our framework. It trains an ideal policy and a dynamics model under the non-perturbative simulation environment. They provide the reference action and the imagined next observation to construct the imagined transition of the ideal gait. After that, the imagined transition should be used to guide the learning of robust policy. We utilized the imagined transition as part of the network input and optimized it via RL. This approach not only increases the training efficiency but also improves the generalization of the locomotion policy. Additionally, the predicted observation from the dynamics model may encounter Out-of-Distribution (OOD) problems due to the distribution shift between the complex and ideal environments. If we include it in the optimization objective, it will lead to training crash or non-convergence. Therefore, we designed an adjustment mechanism of the dynamics model to mitigate the negative impact of OOD observation on policy learning.

In summary, the contributions of our work are as follows:

- We propose **LIT**, an RL-based locomotion training paradigm that includes ideal gait learning and robust policy learning with imagined transitions.
- We develop a method to capture the desired gait in the simulator through joint training of the policy and dynamics model in a non-perturbative simulation environment.
- We introduce a dynamics model with an adjustment mechanism to mitigate the adverse effects of errors in the dynamics model when encountering OOD observations.
- We conduct extensive experiments and ablations in both simulators and real-world scenarios. The empirical results demonstrate that LIT improves training efficiency and enhances performance in both settings.

## II. RELATED WORK

### A. RL-based Legged Locomotion

Reinforcement learning has seen significant progress in quadrupedal locomotion control, largely driven by advances in physics simulators like Mujoco [13] and IsaacGym [14]. This high-fidelity, GPU-accelerated platform allows for efficient RL training by simulating complex environments [15].

To mitigate the uncertainty caused by partial observation, the teacher-student framework [3], [16] was proposed, enabling quadrupedal robots to adapt to unknown terrains and greatly improving locomotion flexibility and robustness. Much of the work [17], [18], [19] has continued in this structure with impressive results. Walk-These-Way [5] proposes a method to improve the generalization of quadrupedal locomotion by training the robot in diverse environments. Another attempt is introducing representational learning, such as [20], [4], [6]. DreamWaQ [4], leverages variational autoencoders (VAE) [21] to learn environmental representations, while HIMloco [6] employs contrastive learning techniques to learn terrain representations, further enhancing the robot’s adaptability to various environments. Recent advances [22], [23] introduce model-based control [24] and adaptive control [25] to improve the interpretability

and robustness of RL-based locomotion. To address the challenges of the sim2real gap, domain randomization has been commonly used [1], [2], [3], [4], [6]. It is a class of methods in which the policy is trained with a wide range of environment parameters and sensor noise to learn behaviors that are robust in this range. However, domain randomization trades optimality for robustness, sometimes leading to an over-conservative policy.

### B. Model-based RL

Model-based Reinforcement Learning (MBRL) distinguishes itself by incorporating a learned dynamics model of the environment, which predicts future states given the current state and action. This allows MBRL methods to plan and use collected data efficiently. Popular frameworks in this area include Dreamer series [26], [27], [28], which uses a learned world model to perform planning in latent space, and TDMPc series [29], [30], which integrates model predictive control to improve sample efficiency. In the legged locomotion tasks, recent MBRL approaches have demonstrated the power of learned dynamics models. DayDreamer [31], inspired by Dreamer, enables effective planning and control for robotic locomotion. PIP-loco [32] also adopts a model-based approach and combines it with model predictive control, re-assembling TDMPc. These methods utilize the learned model for trajectory planning or representation learning, leveraging the learned dynamics model to enhance performance. In contrast to these works, our approach utilizes the dynamics model not for planning or representation, but as a reference to predict the next state, thereby more directly affecting policy learning.

## III. PRELIMINARY

a) *POMDP*: In this study, the environment is modeled as an infinite-horizon partially observable Markov decision process (POMDP), represented by the tuple  $\mathcal{M} = (\mathcal{S}, \mathcal{O}, \mathcal{A}, d_0, p, r, \gamma)$ . The full state  $s \in \mathcal{S}$ , partial observation  $o \in \mathcal{O}$ , and action  $a \in \mathcal{A}$  are all continuous variables. The system begins with an initial state distribution, denoted by  $d_0(s_0)$ , and evolves according to the state transition probability  $p(s_{t+1}|s_t, a_t)$ . Each state transition yields a reward determined by the reward function  $r: \mathcal{S} \times \mathcal{A} \rightarrow \mathcal{R}$ , while the discount factor is specified by  $\gamma \in [0, 1)$ . Additionally, we define a temporal observation at time  $t$  over the previous  $H$  time steps as  $\mathbf{o}_{t-H:t} = [\mathbf{o}_t \ \mathbf{o}_{t-1} \ \cdots \ \mathbf{o}_{t-H}]^T$ . This representation captures the history of partial observations within the temporal window, which is crucial for decision-making in partially observable settings.

b) *State Space*: The policy network takes partial observations  $\mathbf{o}_t$  as input, which consist of the desired velocity, proprioceptive data from the joint encoders and IMU, as well as the previous action  $\mathbf{a}_{t-1}$ . The IMU provides the base angular velocity  $\boldsymbol{\omega}_t$  and the gravity direction in the robot’s frame of reference, denoted by  $\mathbf{g}_t$ . The desired velocity,  $\mathbf{c}_t = [v_x^c, v_y^c, \omega_{yaw}^c]$ , represents the linear velocities in the longitudinal and lateral directions, as well as the angular velocity around the yaw axis. The joint encoders

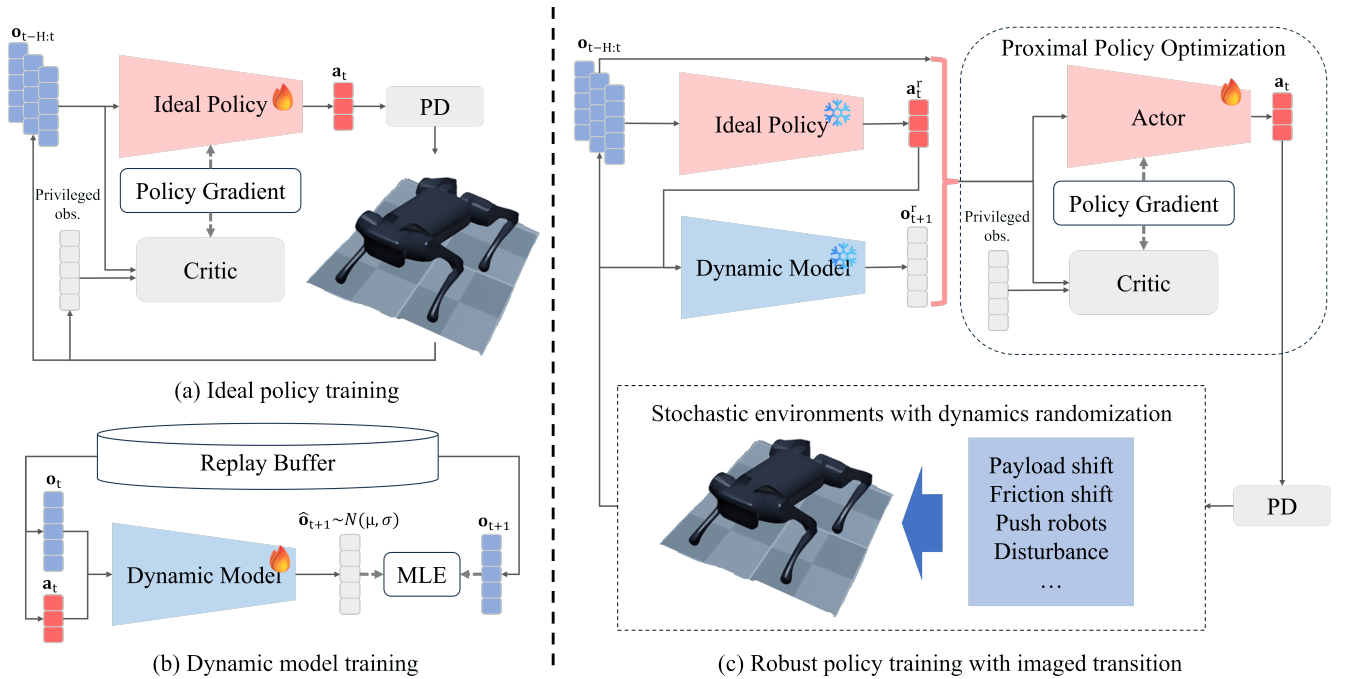


Fig. 2. **Framework Overview of LIT.** The left part is gait reference learning in fixed dynamics. The right part is policy learning with imagined transition.  $\mathbf{a}'_t$  and  $\mathbf{o}'_{t+1}$  mean reference action and imagined next observation respectively.  $[\mathbf{o}_t, \mathbf{a}'_t, \mathbf{o}'_{t+1}]$  constitutes the imagined transition

supply the joint position  $\theta_t$  and the joint velocity  $\dot{\theta}_t$ . In the training phase, the critic network is granted access to privileged information, enabling it to provide more accurate state value estimations. The input to the critic network,  $\mathbf{o}'_t$ , includes three additional components compared to the actor network's input  $\mathbf{o}^a_t$ : the current velocity  $\mathbf{v}_t$ , the external force  $\mathbf{f}_t$ , and the surrounding ground height  $\mathbf{h}_t$ .

c) *Action Space*: The movement of each actuator is modeled as the difference between the target joint position, denoted as  $\theta_{\text{target}}$ , and the nominal joint position,  $\theta_0$ . To mitigate the instability in the network's output, we introduce a scaling factor  $k \leq 1$  that is applied to the policy output  $\mathbf{a}_t$ . Consequently, the final target joint positions are given by the equation:  $\theta_{\text{target}} = \theta_0 + k\mathbf{a}_t$ . The action space  $\mathcal{A}$  is defined by the number of actuators in the system. For instance, in the case of quadrupedal robots such as the Unitree A1, which is equipped with 12 actuators (3 on each leg), the dimension of the action space is 12.

## IV. METHOD

### A. Framework Overview

Our framework is shown in Fig. 2. It is a general approach that can be incorporated into most of the previous RL-based Locomotion methods such as RMA [3], Dreamwaq [4], HIM-LoCo [6], etc., and here we use HIMLoCo as the backbone algorithm. It consists of two parts, Gait Reference Learning and Policy Learning with Imagined Transition. Section IV-B discusses how to perform Gait Reference Learning. It aims to obtain the optimal gait from a fixed simulation environment and compress the optimal gait into an ideal policy and a

dynamics model. Section IV-C presents how to use gait reference to guide policy learning.

### B. Gait Reference Learning in Fixed Dynamics

1) *Ideal Policy*: In the process of reinforcement learning to train robotic policies, we found that the wider ranges of dynamic randomization, the lower returns that can be obtained when the training converges. To obtain an optimal reference, we train a policy that is optimal in the unperturbed simulation environment in a fixed dynamic (i.e., no dynamic randomization setting) environment, which is called the ideal policy  $\pi_{\text{ideal}}(\mathbf{a}'_t | \mathbf{o}_{t:H})$  in the paper.

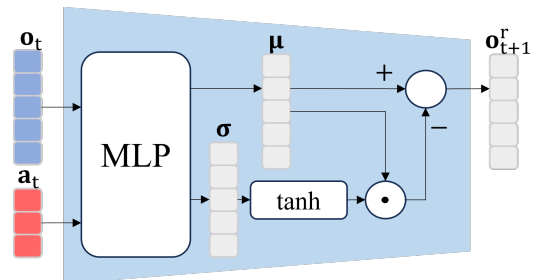


Fig. 3. **Architecture of Dynamics Model.** An adjustment mechanism is added to the output of the dynamics model.

2) *Dynamics Model*: To obtain reference observations, we train a dynamics model under the non-perturbative simulation environment. The output of the dynamics model includes  $\mu$  and  $\sigma$  in 1, which means the mean and standard deviation of the next observation estimation. We sample the observation estimation  $\hat{\mathbf{o}}_{t+1}$  from normal distribution  $N(\mu, \sigma)$  for net-

work optimization. The optimization objective of the dynamics model is the maximum likelihood estimation, represented by the formula 3.

$$\mu, \sigma \sim P(\cdot | \mathbf{o}_t, \mathbf{a}_t) \quad (1)$$

$$\hat{\mathbf{o}}_{t+1} \sim N(\mu, \sigma) \quad (2)$$

$$\mathcal{L}_{MLE} = -\hat{\mathbf{o}}_{t+1} \log(\mathbf{o}_{t+1}) \quad (3)$$

In most model-based methods, model error is an unavoidable problem. We measured prediction error  $\|\mathbf{o}_{t+1} - \mu\|_2$  while applying the unseen disturbance in the robot's body or not, and compared it to  $\sigma$ . The results in Fig. 4 show a strong correlation between actual prediction error and  $\sigma$  given by the learned model.

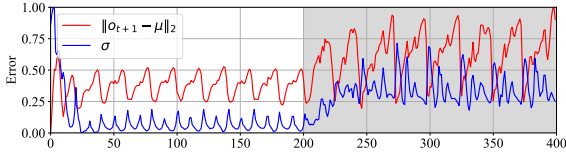


Fig. 4. Correlation between standard deviation estimate and actual observation bias. Unseen disturbance is applied to the robot after 200 steps.

To prevent training and deployment collisions caused by model inaccuracies, we developed an adjustment mechanism to adjust the prediction of the next observation. According to the general law of supervised learning, the larger the standard deviation  $\sigma$  the less reliable the prediction  $\mu$  of the dynamics model. Thus, when the variance is large, we should minimize the effect of the observation reference on the subsequent network. Inspired by [4], [33], we multiply the weight  $(1 - \text{norm}(\sigma)) \in [0, 1]$  dot by  $\mu$  with the following equation 4.

Experiments in 8 showed that this design significantly improved the robot's performance in the unseen region.

$$\mathbf{o}_{t+1}^r \sim f(\mu, \sigma) = (1 - \text{norm}(\sigma)) \cdot \mu \quad (4)$$

### C. Policy Learning with Imagined Transition

In short, the only difference in our policy network is that we are adding the input of action and observation reference, which represents gait reference. The combination of  $\mathbf{o}$ ,  $\mathbf{a}_t^r$ , and  $\mathbf{o}_{t+1}^r$  forms a complete state transition, which is our imagined transition. As shown in the bottom of Fig.5, we concatenate reference action  $\mathbf{a}_t^r$  and imagined next observation  $\mathbf{o}_{t+1}^r$  from the gait reference with proprioceptive observations  $\mathbf{o}_t$ , whereas the baseline, depicted on the top, follows the architecture used in [4], [6].

$$\mathbf{a}_t \sim \pi(\cdot | \mathbf{o}_{t-H:t}, \mathbf{z}, \hat{\mathbf{v}}) \quad (5)$$

$$\mathbf{a}_t \sim \pi(\cdot | \mathbf{o}_{t-H:t}, \mathbf{z}, \hat{\mathbf{v}}, \mathbf{a}_t^r, \mathbf{o}_{t+1}^r) \quad (6)$$

Intuitively, solving in the solution space close to the prior gait information input should be more efficient than searching for the optimal solution directly in the huge solution space. This simple change has resulted in a significant increase in the overall performance of policy learning.

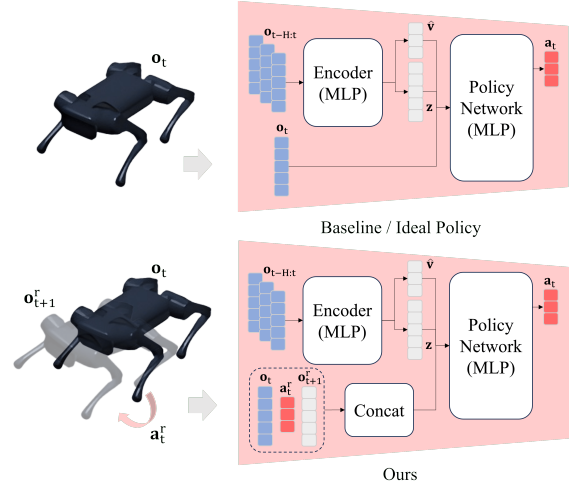


Fig. 5. **Architecture of Policy Network.** The top is the baseline architecture, and the bottom is the architecture of the policy network with imagined transition.

## V. EXPERIMENTS

### A. Experimental Setup

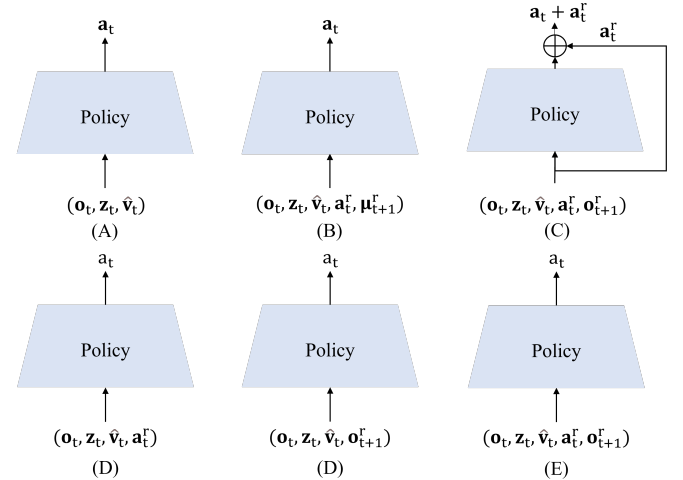


Fig. 6. Compared Methods.

a) *Compared Methods:* To fairly compare our method with others, we set up five variants as Figure 6.

(A) Baseline: Train without observation reference and action reference, equivalent here to [6]; (B) Ours w/o Adjust: Ours without observation reference adjustment, the mean value output from the dynamics model is used directly as the observation reference; (C) Ours w Residual: Action reference is summed with the actor output as action output, similar to [34], [35]; (D) Ours w/o Action Reference: Action reference input is set to zero tensor; (E) Ours w/o State Reference: State reference input is set to zero tensor; (F) Ours;

b) *Simulation Setup:* We use the PPO algorithm with 4096 parallel environments and a rollout length of 100 time steps in Isaac Gym [36]. The training process takes 4096

parallel environments for 2000 iterations in the NVIDIA A800 GPU. In Section V-B.2, we trained longer iterations to observe learning curves.

### B. Evaluation on Simulator

1) *Command Tracking*: We evaluate the tracking errors in linear velocity and angular velocity per second for each algorithm under various terrains. Tracking errors are calculated by  $\|v_{x,y} - v_{x,y}^{\text{target}}\|^2$  and  $\|\omega_{\text{yaw}} - \omega_{\text{yaw}}^{\text{target}}\|^2$  respectively. The results in Table I show that our method has a lower velocity tracking error.

TABLE I  
AVERAGE TRACKING ERROR IN SIMULATOR OVER 1000 TRIALS.

Terrain Types	Velocity Types	Baseline	Ours
Smooth Slopes	Linear	0.170	<b>0.120</b>
	Angular	0.101	<b>0.099</b>
Rough Slopes	Linear	0.387	<b>0.162</b>
	Angular	0.164	<b>0.130</b>
Stairs	Linear	2.371	<b>0.992</b>
	Angular	<b>0.515</b>	0.552
Discrete	Linear	1.955	<b>0.120</b>
	Angular	0.220	<b>0.099</b>

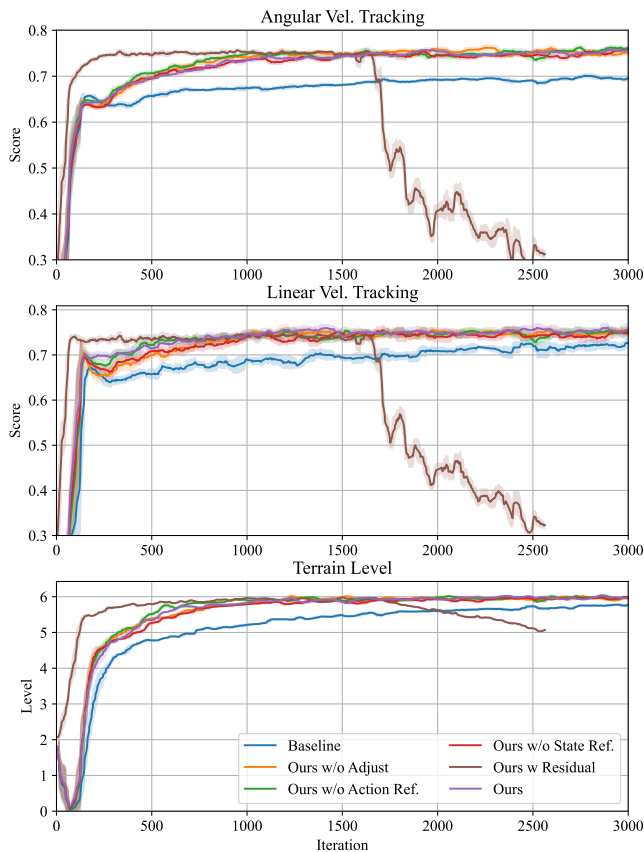


Fig. 7. **Ablation studies with learning curves.** From top to bottom: (1) normalized linear velocity tracking score, (2) normalized angular velocity tracking score, and (3) maximum reachable terrain level in training environments.

2) *Learning Curve*: We recorded the growth of velocity tracking score and terrain passing ability for differ-

ent algorithms during training. The normalized angular velocity tracking score and the normalized linear velocity tracking score are calculated by  $\exp(-\frac{\|\omega_{\text{yaw}} - \omega_{\text{yaw}}^{\text{target}}\|^2}{0.25})$  and  $\exp(-\frac{\|v_{x,y} - v_{x,y}^{\text{target}}\|^2}{0.25})$  respectively. The terrain is categorized into 9 difficulty levels based on the curriculum setting, the same as [6].

Observing from the learning curves in Figure 7, our method consistently maintains an advantage over the baseline in terms of tracking error and terrain traversal ability throughout the training process. Notably, after the introduction of action residual, the method crashed in the middle of training. Based on previous analysis, there is a distribution shift between reference learning and policy learning. Although residual concatenation of reference action of imagined transitions improves the speed of policy learning early in training, the imagined transitions are unreliable when encountering the OOD state, leading to potential policy training breakdowns. Our adjustment mechanism of the dynamics model aims to mitigate the adverse effects of this OOD issue.

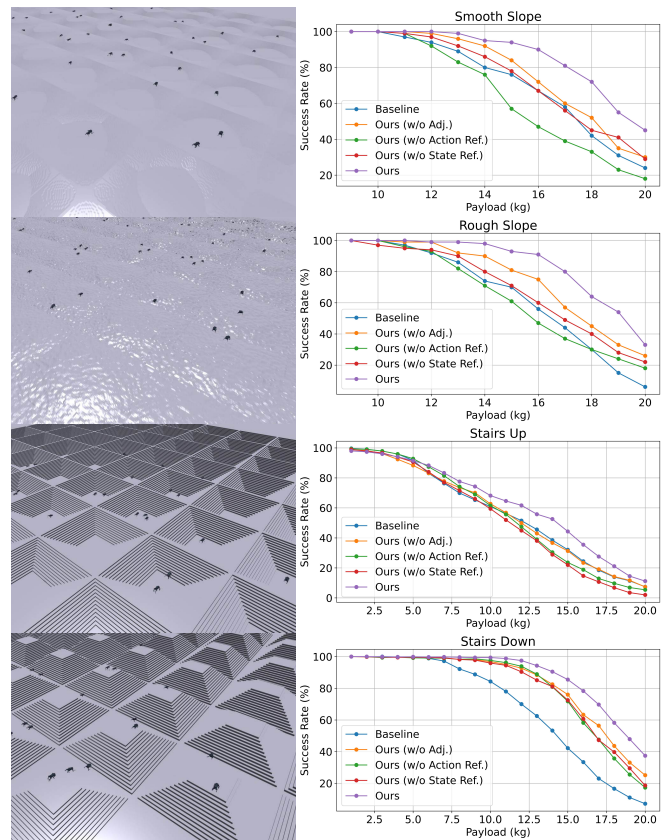


Fig. 8. **Success rate of different algorithms under various payloads.** The success rate for payloads from 1kg to 9kg on both smooth and rough slopes is 100%.

3) *Payload Shift*: To verify the performance of our approach against the unknown heavy payload, we tested the success rate of the A1 robot in executing different payloads on four different terrains: smooth slopes, rough slopes, stairs up, and stairs down with varying levels of difficulty. The robot was required to walk forward with the command [1,



Fig. 9. **Deployment on Real World.** Five scenarios in order from left to right: (1) Plane - flat surface walking, (2) Payload - carrying 3 Kg additional weight, (3) Disturbance-1 - external force applied from the back, (4) Disturbance-2 - external disturbance applied to the right-back leg, and (5) Lawn - walking on uneven grassy terrain.

$0, 0]$ (m/s) in all four terrains for 200 steps. The range of payload gradually increases from 1kg to 20kg. For smooth and rough slopes, we execute 100 times with different seeds, and since the terrain of stairs is more complicated, we execute 1000 times to calculate the success rate, and the result is shown in Figure 8.

On all test terrains, our method survived significantly better than the other compared methods when faced with unseen heavy loads. In addition, we can find that although the changes in state adjustment and action reference input do not show significant differences in the learning curve and the evaluation within the distribution, they affect the performance of the method in unseen payloads.

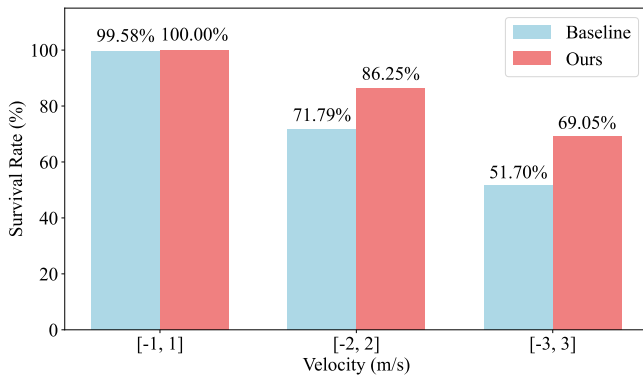


Fig. 10. **Comparison of survival rate under external pushing.** The experimental results are categorized into three classes based on the magnitude of the external push velocity. A higher survival rate indicates better robustness.

4) *Adding push to robots:* Pushing a robot with external force is a widely used method for evaluating the robustness of its locomotion. In this experiment, the push force was applied by adding a random velocity to the quadruped’s base along the  $xy$ -plane of the world frame. The robot was instructed to walk forward with a command of  $[1, 0, 0]$  m/s, while simultaneously responding to the unpredicted random push. The magnitude of the added velocity determines the intensity of the push, with larger magnitudes corresponding to more forceful pushes. To assess the robustness of our approach in comparison to the baseline, pushes were randomly sampled 2000 times within a velocity range of  $[-3, 3]$  m/s. The results in Figure 10 illustrate that our method outperforms the

baseline in terms of fall resistance when subjected to external pushes.

Figure 11 provides a detailed visualization of the standing versus falling status under various push magnitudes and directions for different algorithms. Given the command  $[1, 0, 0]$  m/s, it can be observed that Figure 11 exhibits near-symmetry along the  $x$ -axis, but not along the  $y$ -axis. All methods include push perturbations within the range  $[-1, 1]$  m/s during the robust training phase, and consequently, they perform well within this range. However, as the perturbation range increases, the advantage of our approach becomes increasingly pronounced. Our method outperforms the baseline by surviving more than 300 additional times in 2000 randomized tests.

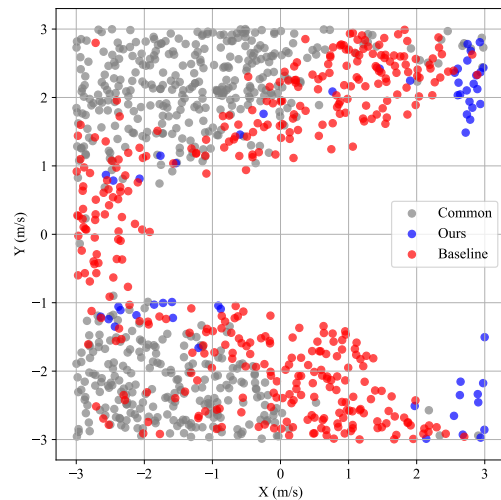


Fig. 11. **Fall resistant visualization with external push.** ‘Common’ represents cases where both ours and baseline fall. ‘Ours’ and ‘Baseline’ represent cases where each falls but the other survives.

### C. Evaluation on Real World

To test the effectiveness of policy deployment in the real world, we designed a variety of challenging scenarios as shown in Figure 9. We deployed the policy for training 2000 iterations on the UniTree A1 robot, with the PD controller’s parameters set to  $Kp = 40.0$  and  $Kd = 1.0$ . The robot was instructed to walk forward with a command of

$[1, 0, 0]$  m/s in five scenarios. We measured the tracking errors  $\|v_{x,y} - v_{x,y}^{target}\|^2$  as the performance metric to evaluate the robot’s ability to track the linear velocity command, where the body velocity  $v_{x,y}$  is collected by the robot’s IMU. The results in Figure 12 show that our method has a lower tracking error in five scenarios compared to the baseline.

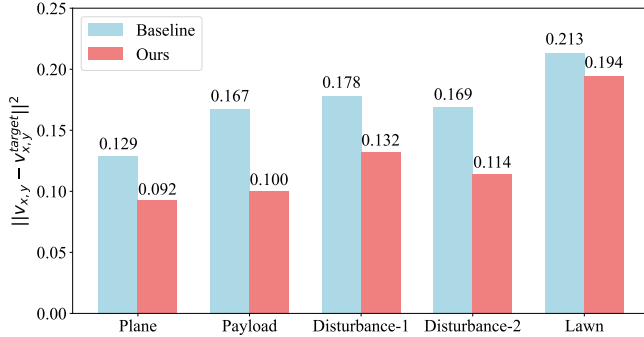


Fig. 12. **Comparison of command tracking performance in real-world scenarios.** The results are averaged over ten trials. A lower tracking error indicates better deployed performance.

#### D. Implementation Details

a) *Reward Design:* The design of reward functions follows previous research[4] and is shown in Table II.

TABLE II  
REWARD FUNCTIONS.

Reward	Equation ( $r_i$ )	Weight ( $w_i$ )
Linear velocity tracking	$\exp\left\{-\frac{\ v_{xy}^{cmd} - v_{xy}\ _2^2}{0.25}\right\}$	1.0
Angular velocity tracking	$\exp\left\{-\frac{(\omega_{yaw}^{cmd} - \omega_{yaw})^2}{0.25}\right\}$	0.5
Lin. velocity ( $z$ )	$v_z^2$	-2.0
Ang. velocity ( $xy$ )	$\ \omega_{xy}\ _2^2$	-0.05
Orientation	$\ \mathbf{g}\ _2^2$	-0.2
Joint accelerations	$\ \ddot{\theta}\ _2^2$	$-2.5 \times 10^{-7}$
Joint power	$ \tau   \dot{\theta} ^T$	$-2 \times 10^{-5}$
Body height	$(h^{target} - h)^2$	-1.0
Foot clearance	$\sum_{i=0}^3 (p_z^{target} - p_z^i)^2 \cdot v_{xy}^i$	-0.01
Action rate	$\ \mathbf{a}_t - \mathbf{a}_{t-1}\ _2^2$	-0.01
Smoothness	$\ \mathbf{a}_t - 2\mathbf{a}_{t-1} + \mathbf{a}_{t-2}\ _2^2$	-0.01

Where  $h^{target}$  is the desired base height corresponding to ground,  $p_z^{target}$  and  $p_z^i$  are the desired feet position and real feet position in the  $z$ -axis of robots’ frame and  $v_{xy}^i$  is the feet velocity in  $xy$ -plane of robot’s frame.

b) *Dynamics Randomization:* We randomize the mass of the robot body and links, the center of mass (CoM) of the robot, the payload applied to the body of the robot, the ground friction and restitution coefficients, the motor strength, the joint-level PD gains, the system delay, the external force, and the initial joint positions during policy Learning with imagined transition. The randomization ranges for each parameter are detailed in Table III.

TABLE III  
DOMAIN RANDOMIZATION.

Parameters	Range	Unit
CoM	$[-0.05, 0.05]$	m
Payload Mass	$[-1, 2]$	Kg
Ground Friction	$[0.2, 1.25]$	-
Motor Strength	$[0.9, 1.1] \times \text{motor torque}$	Nm
Joint $K_p$	$[0.9, 1.1] \times 40.0$	Nm/rad
Joint $K_d$	$[0.9, 1.1] \times 1.0$	Nms/rad
Initial Joint Positions	$[0.5, 1.5] \times \text{nominal value}$	rad
System Delay	$[0, 15]$	ms
External Force	$[-30, 30]$	N

c) *Training Curriculum:* To facilitate robot learning, we adopt a terrain curriculum and command curriculum inspired by the approaches of [36], [37], and [6]. Specifically, we construct a height field map comprising 200 distinct terrains organized in a  $20 \times 10$  grid. Within each row, terrains are arranged in increasing order of difficulty, and each grid cell measures  $10 \times 10 m^2$ . Initially, robots are placed on the simplest terrain types. As the robot’s performance improves, the terrain difficulty level increases once the robot achieves at least 80% of the linear tracking reward. Conversely, the difficulty decreases if the robot cannot traverse half of the terrain within a single episode. For terrains involving stairs or discrete obstacles, we sample longitudinal and lateral linear velocity commands from the range  $[-1.0, 1.0]$  m/s and the horizontal angular velocity from  $[-2.0, 2.0]$  rad/s. For slopes and rough terrains, the range of longitudinal linear velocity is extended to  $[-3.0, 3.0]$  m/s, and the range for horizontal angular velocity is expanded to  $[-3.0, 3.0]$  rad/s. All commands are sampled independently for each robot from the specified ranges, with sampling occurring every 25-time steps.

## VI. CONCLUSION

In this paper, We propose LIT, a two-stage framework that mitigates the trade-off between robustness and optimality in RL-based locomotion. By introducing an imagined transition to policy learning, LIT enables policies trained with domain randomization to be guided by the desired gait in the simulator. Extensive experiments demonstrate significant improvements in velocity tracking under both simulators and real-world environments. LIT provides a new training paradigm when a large amount of domain randomness needs to be used for robustness. In future work, we will continue to investigate robotic scenarios exhibiting inherent trade-offs between precision and robustness, while exploring generalized implementations of this paradigm across broader application domains.

## ACKNOWLEDGMENT

This work was supported by the National Science and Technology Innovation 2030-Major Projects (Grant No. 2022ZD0208800) and the National Natural Science Foundation of China (Grant No. 62176215 and 62003018).

## REFERENCES

- [1] Z. Xie, X. Da, M. van de Panne, B. Babich, and A. Garg, "Dynamics randomization revisited: A case study for quadrupedal locomotion," in *Proc. IEEE International Conference on Robotics and Automation (ICRA)*, 2021, pp. 4955–4961.
- [2] J. Tan, T. Zhang, E. Coumans, A. Iscen, Y. Bai, D. Hafner, S. Bohez, and V. Vanhoucke, "Sim-to-real: Learning agile locomotion for quadruped robots," *arXiv preprint arXiv:1804.10332*, 2018.
- [3] A. Kumar, Z. Fu, D. Pathak, and J. Malik, "Rma: Rapid motor adaptation for legged robots," in *Robotics: Science and Systems*, 2021.
- [4] I. M. A. Nahrendra, B. Yu, and H. Myung, "Dreamwaq: Learning robust quadrupedal locomotion with implicit terrain imagination via deep reinforcement learning," in *IEEE International Conference on Robotics and Automation (ICRA)*, 2023.
- [5] G. B. Margolis and P. Agrawal, "Walk these ways: Tuning robot control for generalization with multiplicity of behavior," in *Conference on Robot Learning (CoRL)*, 2023.
- [6] J. Long, Z. Wang, Q. Li, L. Cao, J. Gao, and J. Pang, "Hybrid internal model: Learning agile legged locomotion with simulated robot response," in *The Twelfth International Conference on Learning Representations*, 2024.
- [7] J. Tobin, R. Fong, A. Ray, J. Schneider, W. Zaremba, and P. Abbeel, "Domain randomization for transferring deep neural networks from simulation to the real world," in *2017 IEEE/RSJ international conference on intelligent robots and systems (IROS)*. IEEE, 2017, pp. 23–30.
- [8] Y. Bengio, J. Louradour, R. Collobert, and J. Weston, "Curriculum learning," in *Proceedings of the 26th annual international conference on machine learning*, 2009, pp. 41–48.
- [9] B. Mehta, M. Diaz, F. Golemo, C. J. Pal, and L. Paull, "Active domain randomization," in *Proceedings of the Conference on Robot Learning*, ser. Proceedings of Machine Learning Research, L. P. Kaelbling, D. Kragic, and K. Sugiura, Eds., vol. 100. PMLR, 30 Oct–01 Nov 2020, pp. 1162–1176. [Online]. Available: <https://proceedings.mlr.press/v100/mehta20a.html>
- [10] G. Tiboni, P. Klink, J. Peters, T. Tommasi, C. D'Ermo, and G. Chaltatzaki, "Domain randomization via entropy maximization," 2023.
- [11] M. T. Spaan, "Partially observable markov decision processes," in *Reinforcement learning: State-of-the-art*. Springer, 2012, pp. 387–414.
- [12] H. Kurniawati, "Partially observable markov decision processes and robotics," *Annual Review of Control, Robotics, and Autonomous Systems*, vol. 5, no. 1, pp. 253–277, 2022.
- [13] E. Todorov, T. Erez, and Y. Tassa, "Mujoco: A physics engine for model-based control," in *2012 IEEE/RSJ international conference on intelligent robots and systems*. IEEE, 2012, pp. 5026–5033.
- [14] V. Makoviychuk, L. Wawrzyniak, Y. Guo, M. Lu, K. Storey, M. Macklin, D. Hoeller, N. Rudin, A. Allshire, A. Handa, *et al.*, "Isaac gym: High performance gpu-based physics simulation for robot learning," *Advances in neural information processing systems*, 2021.
- [15] N. Rudin, D. Hoeller, P. Reist, and M. Hutter, "Learning to walk in minutes using massively parallel deep reinforcement learning," 2022. [Online]. Available: <https://arxiv.org/abs/2109.11978>
- [16] J. Lee, J. Hwangbo, L. Wellhausen, V. Koltun, and M. Hutter, "Learning quadrupedal locomotion over challenging terrain," *Science Robotics*, vol. 5, no. 47, p. eabc5986, 2020. [Online]. Available: <https://www.science.org/doi/abs/10.1126/scirobotics.abc5986>
- [17] A. Agarwal, A. Kumar, J. Malik, and D. Pathak, "Legged locomotion in challenging terrains using egocentric vision," in *Proceedings of The 6th Conference on Robot Learning*, ser. Proceedings of Machine Learning Research, K. Liu, D. Kulic, and J. Ichnowski, Eds., vol. 205. PMLR, 14–18 Dec 2023, pp. 403–415. [Online]. Available: <https://proceedings.mlr.press/v205/agarwal23a.html>
- [18] X. Cheng, K. Shi, A. Agarwal, and D. Pathak, "Extreme parkour with legged robots," in *2024 IEEE International Conference on Robotics and Automation (ICRA)*, 2024, pp. 11 443–11 450.
- [19] A. Kumar, Z. Li, J. Zeng, D. Pathak, K. Sreenath, and J. Malik, "Adapting rapid motor adaptation for bipedal robots," in *2022 IEEE/RSJ International Conference on Intelligent Robots and Systems (IROS)*. IEEE, 2022, pp. 1161–1168.
- [20] G. Ji, J. Mun, H. Kim, and J. Hwangbo, "Concurrent training of a control policy and a state estimator for dynamic and robust legged locomotion," *IEEE Robotics and Automation Letters*, vol. 7, no. 2, pp. 4630–4637, 2022.
- [21] I. Higgins, L. Matthey, A. Pal, C. Burgess, X. Glorot, M. Botvinick, S. Mohamed, and A. Lerchner, " $\beta$  - VAE: Learning basic visual concepts with a constrained variational framework," in *Proc. International Conference on Learning Representations (ICLR)*, 2017.
- [22] S. Lyu, H. Zhao, and D. Wang, "A composite control strategy for quadruped robot by integrating reinforcement learning and model-based control," in *2023 IEEE/RSJ International Conference on Intelligent Robots and Systems (IROS)*. IEEE, 2023, pp. 751–758.
- [23] S. Lyu, X. Lang, H. Zhao, H. Zhang, P. Ding, and D. Wang, "RI2ac: Reinforcement learning-based rapid online adaptive control for legged robot robust locomotion," in *Proceedings of the Robotics: Science and Systems*, 2024.
- [24] D. Kim, J. Di Carlo, B. Katz, G. Bledt, and S. Kim, "Highly dynamic quadruped locomotion via whole-body impulse control and model predictive control," *arXiv preprint arXiv:1909.06586*, 2019.
- [25] P. A. Ioannou and J. Sun, *Robust adaptive control*. PTR Prentice-Hall Upper Saddle River, NJ, 1996, vol. 1.
- [26] D. Hafner, T. Lillicrap, J. Ba, and M. Norouzi, "Dream to control: Learning behaviors by latent imagination," *arXiv preprint arXiv:1912.01603*, 2019.
- [27] D. Hafner, T. Lillicrap, M. Norouzi, and J. Ba, "Mastering atari with discrete world models," *arXiv preprint arXiv:2010.02193*, 2020.
- [28] D. Hafner, J. Pasukonis, J. Ba, and T. Lillicrap, "Mastering diverse domains through world models," *arXiv preprint arXiv:2301.04104*, 2023.
- [29] N. Hansen, X. Wang, and H. Su, "Temporal difference learning for model predictive control," *arXiv preprint arXiv:2203.04955*, 2022.
- [30] N. Hansen, H. Su, and X. Wang, "Td-mpc2: Scalable, robust world models for continuous control," *arXiv preprint arXiv:2310.16828*, 2023.
- [31] P. Wu, A. Escontrela, D. Hafner, P. Abbeel, and K. Goldberg, "Daydreamer: World models for physical robot learning," in *Conference on Robot Learning (CoRL)*, 2023.
- [32] A. Shirwatkar, N. Saxena, K. Chandra, and S. Kolathaya, "Pip-loco: A proprioceptive infinite horizon planning framework for quadrupedal robot locomotion," *arXiv preprint arXiv:2409.09441*, 2024.
- [33] I. Nahrendra, B. Yu, M. Oh, D. Lee, S. Lee, H. Lee, H. Lim, and H. Myung, "Obstacle-aware quadrupedal locomotion with resilient multi-modal reinforcement learning," *arXiv preprint arXiv:2409.19709*, 2024.
- [34] T. Silver, K. Allen, J. Tenenbaum, and L. Kaelbling, "Residual policy learning," *arXiv preprint arXiv:1812.06298*, 2018.
- [35] X. Yuan, T. Mu, S. Tao, Y. Fang, M. Zhang, and H. Su, "Policy decorator: Model-agnostic online refinement for large policy model," *arXiv preprint arXiv:2412.13630*, 2024.
- [36] N. Rudin, D. Hoeller, P. Reist, and M. Hutter, "Learning to walk in minutes using massively parallel deep reinforcement learning," in *Conference on Robot Learning (CoRL)*, 2022.
- [37] J. Wu, G. Xin, C. Qi, and Y. Xue, "Learning robust and agile legged locomotion using adversarial motion priors," *IEEE Robotics and Automation Letters*, 2022.